Sustainable Chemical Engineering
https://ojs.wiserpub.com/index.php/SCE/

UNIVERSAL WISER PUBLISHER

Research Article

Enhancing Barrier and Mechanical Performance of Recycled HDPE and Renewable Origin PP Composites Using Slate and Bivalve Shell Mineral Fillers for Green Packaging

Bruna Basto[1*], Bárbara Freitas[1], Fernando Leite[1], João Bessa[1], Gonçalo Oliveira[2], Ricardo Neto[3], Raul Fangueiro[1,4]

[1]Fibrenamics-Institute for Innovation in Fibrous and Composite Materials, University of Minho, Guimarães, Portugal
[2]B4Logic, Rua Principal No. 172, Edifício Prisma, 1º D, Ponte de Vagos, 3840-326, Portugal
[3]MPlastic, Rua Principal No. 172, Edifício Prisma, Sala D, Ponte de Vagos, 3840-326, Portugal
[4]Department of Textile Engineering, University of Minho, Guimarães, Portugal
E-mail: brunabasto@fibrenamics.com

Received: 13 November 2025; **Revised:** 21 January 2026; **Accepted:** 28 January 2026

Abstract: The development of sustainable polymer composites requires the integration of renewable or waste-derived fillers that improve performance without compromising processability. In this study, Slate Powder (SP) and Bivalve Shells (BS) were evaluated as alternative mineral reinforcements (5, 10, 20, and 30% (w/w)) for partially recycled High-Density Polyethene (HDPE) and renewable-origin Polypropylene (PP) composites used in packaging applications produced through blow molding extrusion. Mechanical analysis showed that BS increased Young's modulus, while SP preserved flexibility and maintained mechanical properties close to those of fossil-based polymers. No significant influence was observed in rheology (Melt Flow Rate (MFR)). Importantly, both SP and BS enhanced barrier performance by reducing air and water vapour permeability. Ultraviolet (UV) transmittance tests confirmed that SP was highly efficient, achieving near 0% transmittance with only 5% incorporation, while BS required higher loadings (30%) to achieve similar results. When compared to reference materials, all composites exhibited superior barrier properties, underscoring their potential in packaging applications. The approach here described not only supports the circular economy but also offers a viable path to produce high-performance and sustainable polyolefin-based packaging materials.

***Keywords*:** mineral residue, compounding, biocomposites, water vapor barrier, Ultraviolet (UV) resistance, circular economy

1. Introduction

The global demand for plastic materials continues to increase, particularly in the packaging industry, which accounts for an important percentage of the overall utilization of plastic.[1] Conventional packaging materials, predominantly derived from fossil resources, are major contributors to environmental pollution through greenhouse gas emissions and the accumulation of non-biodegradable waste.[2]

Petroleum-based polymers, such as Polypropylene (PP) and Polyethylene (PE), two widely used polyolefins, account for approximately 50% of global polymer production. They are employed in a variety of industrial applications,

DOI: https://doi.org/10.37256/sce.7120269160

from packaging to automotive and aeronautical components, due to their excellent mechanical properties, ease of processing, and affordability.[3] However, there are significant environmental risks related to their widespread use. The inherent non-biodegradability of these polymers leads to their accumulation in natural ecosystems and the production of greenhouse gas emissions.[4]

Therefore, industry and academia have intensified their efforts to develop alternative materials that combine environmental sustainability with comparable or improved performance. The use of recycled polymers and bio-based polymers supplemented with mineral or bio-based fillers has drawn particular interest among these alternatives. Recycled polymers give post-consumer plastics a second life, reduce waste generation, and lower the demand for virgin polymers. Natural fillers and polymers of renewable origin also help to reduce the carbon footprint and dependency on fossil fuels.[5] The incorporation of waste-derived reinforcements significantly enhances polymer composites by promoting circular economic practices and allowing for tailored mechanical, rheological, and barrier properties.[6,7] This strategy not only effectively uses waste resources but also contributes to material sustainability. Such solutions enable the development of sustainable materials that match the performance requirements of packaging applications while also addressing pressing environmental issues.

Recycled plastics often exhibit inferior mechanical and barrier properties compared to their virgin counterparts, while renewable-based polymers, such as PP, face limitations mainly associated with higher production costs. In this context, the incorporation of mineral residues, such as Slate Powder (SP) and Bivalve Shells (BS), emerges as a promising strategy to enhance the performance of recycled High-Density Polyethene (HDPE) and renewable PP while partially offsetting material costs, without compromising their sustainability profile. In this work, it is hypothesized that SP and BS fillers can enhance the structural, rheological, and barrier performance of recycled HDPE and renewable PP composites, thereby supporting the development of high-performance and environmentally friendly packaging solutions.

The present study explores the formulation and characterization of recycled HDPE and renewable PP composites reinforced with SP and BS powder. The developed materials were subjected to mechanical and rheological testing to verify their structural performance and processability, as well as barrier testing to determine their suitability for moisture and gas packaging applications.

Therefore, this research aims to evaluate the potential of SP and BS-reinforced polyolefins as alternatives to traditional packaging materials, thereby contributing to the development of high-performance and environmentally friendly plastic solutions.

2. Materials and methods

2.1 *Materials*

HDPE Repsol Reciclex® 50RX5503, containing 50% post-consumer recycled content from industrial packaging, was supplied by Quimidroga, Portugal. The biobased PP (Bornewables™, Borealis) was provided by Nexeo Plastics. Bondyram 5108 and Bondyram 1101 were purchased from IMCD, Portugal.

SP was kindly donated by a company from the center region of Portugal. BS were obtained from Ria de Aveiro, Portugal. According to literature, the mineralogical composition of SP is mainly, phyllosilicates (mica 22% and chlorite 11%), quartz (35%) and feldspars (32%)[8] and BS is mainly composed by calcium carbonate with a crystalline structure that varies from different percentages of aragonite/calcite to 100% calcite.[9-11]

Both BS and SP were dried at 60 °C for 12 hours and then processed in a jaw crusher. Afterwards, the ground BS and SP were sieved to separate particles smaller than 250 µm.

2.2 *Development of recycled HDPE and renewable origin PP composites reinforced with SP and BS*

2.2.1 *Extrusion*

SP and BS were added, separately, to HDPE and PP formulations at concentrations of 5, 10, 20, and 30% (w/w) to produce compoundings. In the different compositions, the compatibilizer agents were maintained at a concentration of 3% (w/w of total formulation weight). Bondyram 5108 was used in the formulations of HDPE and Bondyram 1101 in the PP formulations.

A twin-screw extruder Tecnocanto TECN-20-LD 44, with a screw diameter of 22 mm and a screw diameter/length ratio of LD 44, was used to produce the compositions. From zone 1 to zone 6, the temperature profile used was 185, 185, 175, 170, 160, and 150 °C, respectively. The feeding and extrusion speeds were 40 rpm and 80 rpm, respectively. After extrusion, the obtained filaments were cooled in a cold-water bath and milled into pellets.

2.2.2 *Compression molding*

The compounds obtained were used to produce 3 mm thick plates and films with thicknesses ranging from 0.6 to 1 mm, using a hot compression molding machine (Fontijne Presses LMP 020) at 200 °C for 15 minutes. The plates and films produced were used to obtain samples for different analyses.

2.3 *Determination of mechanical, rheological, and barrier properties of recycled HDPE and renewable origin PP composites reinforced with SP and BS*

2.3.1 *Tensile properties*

Specimens of type 1 BA used in tensile tests were obtained according to the ISO 527-2 standard.[12] The tensile test was conducted on a 100 kN Hounsfield dynamometer at a rate of 5 mm/min using a 2.5 kN load cell and a gauge length specified in the standard. Five specimens were tested for each formulation of HDPE and PP reinforced with 5, 10, 20 and 30% SP and BS. The test was performed until the rupture or the force decreased significantly. Figure 1 shows examples of the specimens used in the tensile test.

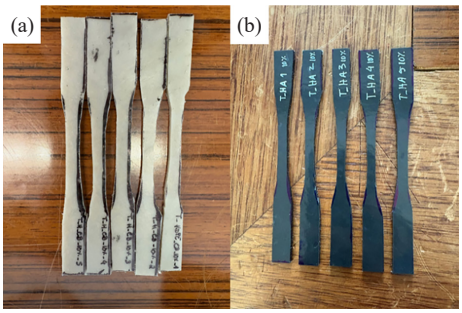

Figure 1. Illustration of the specimens used in the tensile test: a) Bivalve Shells (BS) and b) Slate Powder (SP)

2.3.2 *Flexural properties*

Specimens were obtained according to the ISO 178 standard.[13] The flexural test was performed on the same apparatus as the tensile test, using the same load cell. The gauge length for the test is specified in the standard. Figure 2 presents an example of specimens obtained and used in this test.

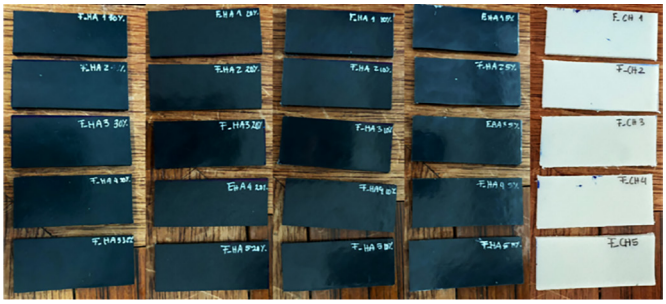

Figure 2. Illustration of the specimens used in the flexural test

2.3.3 *Melt Flow Rate (MFR)*

The Melt Flow Rate (MFR) of the polymer samples was determined according to Procedure A (mass-measurement method) of the ISO 1133-1:2022 standard.[14] The test conditions were selected based on the type of polymer. For HDPE-based samples, the test was conducted at 190 °C under a load of 2.16 kg. For PP-based samples, the test was performed at 230 °C with a load of 2.16 kg.

A standard die with a nominal diameter of 2.095 mm and a length of 8.000 mm was used in all tests. The cutting time intervals varied according to the sample type: 240 seconds for HDPE-based samples and 20 seconds for PP-based samples.

No stabilization or preconditioning of the test specimens was necessary. All measurements were performed in duplicate for each sample to ensure reliability and reproducibility of the results.

2.3.4 *Air permeability test*

The air permeability was measured using an air permeability tester from TEXTEST instruments (Zurich, Switzerland, model FX 3300 with a differential pressure of 100 Pa and a test area of 20 cm^2, adapted from Pais et al.[15] For each sample, at least 10 measurements were taken, and the mean and standard deviation, expressed in $L/m^2 \cdot s$, were calculated.

2.3.5 *Water vapor transmission rate*

Water Vapor Transmission rate (WVT) was determined using a water vapor transmission tester adapted to the E96/E96M-14 standard.[16] Measurements were performed after a one-hour stabilization period and at 24 h. The essay was performed at ambient temperature (ca. 25 °C) and humidity (ca. 50% relative humidity). Three replicates were performed per sample, and the test was performed on several days for each replicate to assess the reproducibility of the results. The mean and standard deviation were determined, and WVT was calculated according to the equation:

$$WVT\left(\frac{\frac{g}{m^2}}{day}\right) = \frac{24 \times m}{A \times t}.$$

Where m corresponds to the mass lost (g), A to the exposed area of the sample (approximately 0.00636 m^2), and t to the time between weighing (t = 24 h).

The samples used in this test had thicknesses of 0.6-1 mm. Figure 3 represents the samples used in this test. For direct comparison, a standard fabric for the water vapor permeability test was used.

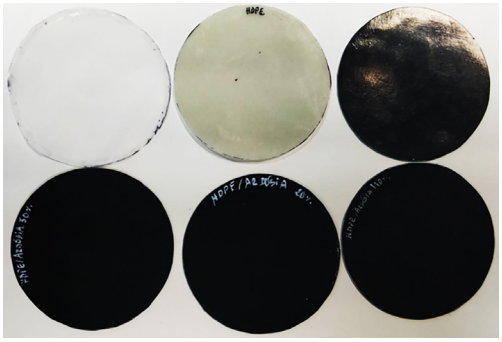

Figure 3. Illustration of the specimens used in the water vapor transmission rate test

2.3.6 *Ultraviolet (UV)-radiation permeability test*

The Ultraviolet (UV)-radiation Permeability (UVP) test of the various formulations was performed in a spectrophotometer. UVP was evaluated by measuring the transmittance from 280 to 400 nm according to the American Society for Testing and Materials (ASTM) E903-20 standard.[17] Samples with thicknesses of 0.6-1 mm and dimensions of 5 × 5 cm were used (Figure 4).

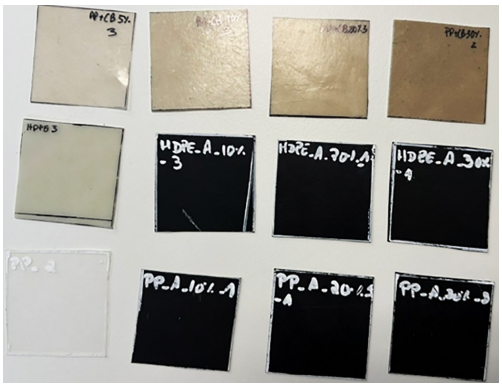

Figure 4. Illustration of the specimens used in the UV-radiation permeability test

2.4 *Scanning Electron Microscopy (SEM)*

The specimen's morphology evaluation was made using the Scanning Electron Microscopy (SEM), a widely employed technique in scientific research for visualizing material morphology at micro and nanoscale levels. SEM utilizes an electron beam to generate high-resolution images of the sample surface. In this study, SEM analysis was conducted on specific areas of different specimens using an Field Electron and Ion (FEI) Nova 200 SEM instrument (Hillsboro, OR, USA).

2.5 *Fourier Transform Infrared Spectroscopy (FTIR)*

The materials' chemical composition was assessed utilizing Fourier Transform Infrared Spectroscopy (FTIR) coupled with the Attenuated Total Reflection (ATR) technique, employing SHIMADZU-IRAffinity-1S instrumentation (Kyoto, Japan). Spectra acquisition was conducted in transmittance mode, encompassing 45 scans across a wavenumber range from 4,000 to 400 cm^{-1}.

2.6 *Proof of concept*

Blow-extruded bottles were produced using formulations of HDPE and PP reinforced with Slate Particles (SP) and Bivalve Shells (BS). The polymer blends were prepared and processed following internal protocols, which cannot be disclosed in detail. Preliminary evaluations focused on the feasibility of the reinforced formulations for extrusion-blow molding, assessing their structural integrity and surface characteristics relevant to packaging applications.

2.7 *Statistical analysis*

Statistical analyses were performed using GraphPad Prism version 10.6.1 (GraphPad Software, San Diego, CA, USA) comparing the new formulations with the respective virgin polymer. Data are presented as mean ± standard deviation. Statistical significance was set at $p < 0.05$.

3. Results and discussion

3.1 *Determination of mechanical, rheological, and barrier properties of recycled HDPE and renewable origin PP composites reinforced with SP and BS*

3.1.1 *Tensile properties*

To evaluate the mechanical properties of the reinforced composites, the Young's modulus (GPa) of all PP and HDPE samples reinforced with SP and BS was evaluated using the force (N) and extension (mm) measured through the dynamometer. The Young's modulus values were calculated for each formulation and are presented in Figure 5.

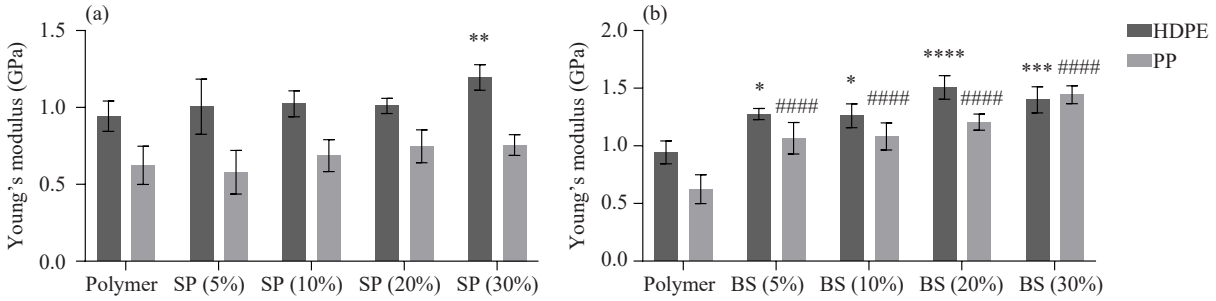

Figure 5. Young's modulus (GPa) for different formulations of PP and HDPE with and without reinforcement in 5, 10, 20 and 30% (w/w) of a) Slate Powder (SP) and b) Bivalve Shells (BS). Values are the mean ± SD (n = 5). Statistical analysis was performed using two-way Analysis of Variance (ANOVA) Dunnett's multiple comparisons test (*p < 0.05; **p < 0.01; ***p < 0.001; ****p < 0.0001; ####p < 0.0001)

Figure 5a shows that the recycled HDPE formulation had a Young's modulus of 0.94 GPa, and the biobased PP 0.62 GPa. The Young's modulus does not vary significantly by up to 30% for both polymers when SP is incorporated. At 30% an increase in this parameter translates into an increase in stiffness in HDPE and no significant difference were observed in PP.

This finding contrasts with existing literature,[18] suggesting that the incorporation of SP into this HDPE does not compromise its mechanical integrity until 30%.

In the present work, the addition of SP to both HDPE and PP does not impact the mechanical integrity of the initial polymers until 20%. This is a noteworthy finding, especially for applications that require the preservation of these properties, such as blow extrusion for packaging production. This result may be explained by the low intrinsic reinforcement efficiency of the slate powder related to its geometry (shape factor). Slate powder is generally composed of irregular or near-spherical particles, which translates to a low aspect ratio. The elastic modulus is highly dependent on the filler's geometry, requiring a high aspect ratio for effective stress transfer and significant stiffening. Particles with a low aspect ratio are intrinsically poor at reinforcing rigidity, even when the polymer-filler interface is chemically improved by a coupling agent. Consequently, the low shape factor may have limited the mineral's ability to efficiently carry the mechanical load, resulting in negligible stiffening of the PP or HDPE matrix.

In Figure 5b, the Young's modulus values for the formulations containing added BS indicate that Young's modulus increases as the percentage of BS rises for HDPE. For PP, the lowest addition of BS results in greater significant differences. Thus, all developed formulations exhibit statistically significant differences when compared to their corresponding virgin polymer samples. This effective stiffening is attributed to the optimized fineness and surface chemistry of the biogenic calcium carbonate that compose BS, which allows for excellent dispersion and superior interfacial stress transfer compared to other low aspect ratio mineral fillers. These findings are in concordance with the existing literature, as the incorporation of mineral particles typically leads to an increase in Young's modulus.[19,20]

Overall, the Young's modulus results indicate that the incorporation of mineral fillers can be tailored to either preserve or enhance the stiffness of HDPE and PP, depending on the filler type and content. The absence of significant changes in stiffness up to 20% SP is particularly relevant for processing technologies commonly used in packaging applications, such as blow extrusion, where maintaining the mechanical integrity of the base polymer is essential. In contrast, the consistent increase in Young's modulus observed for BS-filled systems demonstrates an effective

reinforcing behavior, leading to stiffness levels that fall within or above the range typically required for rigid packaging materials. These findings highlight the distinct roles of filler morphology and surface chemistry in governing mechanical performance and underscore the potential of the developed formulations to meet industrial mechanical expectations without compromising processability.

3.1.2 *Flexural properties*

During the flexural test, it was observed that the specimens deformed but did not rupture (Figure 6). As a result, the test was stopped when the force value dropped significantly.

Figure 6. Illustration of the deformed specimens in the flexural test

The flexural modulus (GPa) of HDPE and PP formulations reinforced with different percentages of SP and BS (5, 10, 20 and 30%) was determined and compared with the flexural modulus obtained for HDPE and PP without reinforcement (Figure 7).

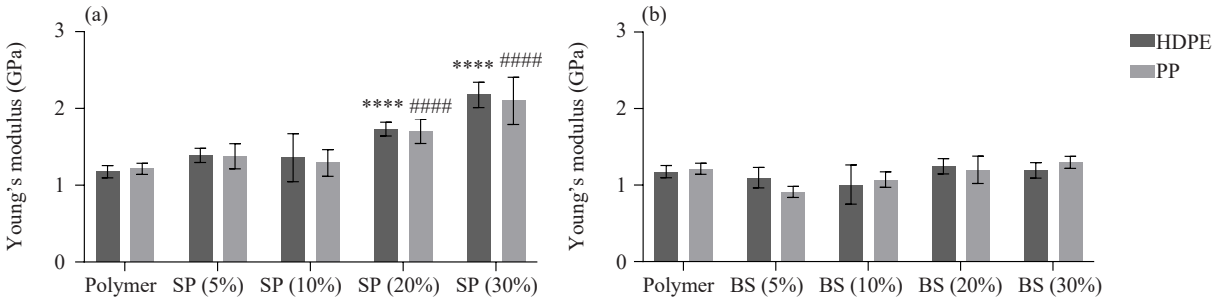

Figure 7. Flexural modulus (GPa) for different formulations of PP and HDPE with and without reinforcement in 5, 10, 20 and 30% (w/w) of a) Slate Powder (SP) and b) Bivalve Shells (BS). Values are the mean ± SD (n = 5). Statistical analysis was performed using two-way ANOVA Dunnett's multiple comparisons test (****$p < 0.0001$; ####$p < 0.0001$)

Recycled HDPE and biobased PP obtained a flexural modulus of 1.18 and 1.21 GPa, respectively (Figure 7). Figure 7a shows the effect of SP incorporation on the flexural modulus. For both HDPE and PP, a significant increase in stiffness is observed from 20% SP incorporation, compared to virgin polymers. Overall, these results indicate that SP incorporation enhances the flexural stiffness of both HDPE and PP.

Figure 7b presents the flexural modulus of composites reinforced with BS. For both HDPE and PP, the flexural modulus approaches that of the virgin polymer, with no significant differences observed in all the formulations tested.

These findings suggest that SP has a stronger influence on flexural properties than BS, contrary to Young's modulus results. The result aligns with the composition of the fillers. SP contains rigid minerals such as quartz, micas, and chlorite that contribute to increased stiffness.[21] In contrast, BS is primarily composed of calcium carbonate ($CaCO_3$), which is more fragile and results in a lesser impact on flexural properties.[22]

From our knowledge, the flexural performance of the developed materials is comparable to that of polymers conventionally used in the packaging industry. In the case of PP, the flexural modulus of the biobased polymer and its SP-reinforced composites is noticeably higher than typical values reported for commercial PP grades used in rigid packaging (≈ 0.85 GPa), indicating enhanced stiffness. Recycled HDPE exhibits a flexural modulus close to that commonly required for HDPE packaging applications (≈ 1.2 GPa), while SP incorporation enables stiffness levels that meet or exceed these benchmarks. These results demonstrate that the proposed composites could align with the requirements of commercially established packaging materials, supporting their potential for industrial implementation.

The increase in flexural modulus obtained in the present results may be advantageous in packaging materials that require higher dimensional stability and resistance to bending during handling, storage, and transport. However, it should also be noted that excessive stiffening can reduce toughness and flexibility, which highlights the importance of balancing filler content to achieve optimal performance for the intended end use.

3.1.3 *MFR*

MFR values have been determined for samples with 5 and 20% added reinforcement to investigate the effect of increasing the concentration of these fillers on this property. The results are presented in Table 1.

Table 1. Melt flow rate for formulations of HDPE and PP with 5 and 20% of Slate Slate Powder (SP) and Bivalve Shells (BS)

Formulations	Assay conditions	MFR (g/10 min)
HDPE + SP (5%)	190 °C, 2.16 kg	0.30 ± 0.02
HDPE + SP (20%)		0.29 ± 0.02
PP + SP (5%)	230 °C, 2.16 kg	2.60 ± 0.20
PP + SP (20%)		2.39 ± 0.18
HDPE + BS (5%)	190 °C, 2.16 kg	0.25 ± 0.02
HDPE + BS (20%)		0.26 ± 0.02
PP + BS (5%)	230 °C, 2.16 kg	2.49 ± 0.19
PP + BS (20%)		2.42 ± 0.19

No measurable differences were found in the formulations of HDPE and PP with SP reinforcement, suggesting that the increased incorporation of SP into the polymers does not affect the MFR value at the analyzed concentrations. The same result was observed in a polymer reinforced with BS.

The influence of mineral fillers on the melt flow rate of polymers is a nuanced topic, with varying effects depending on the type and amount of filler used. Research indicates that small quantities of fillers can enhance flow properties,[23] while excessive amounts may lead to increased viscosity and processing challenges.[24] This transition can be explained by a plasticizing effect observed at low concentrations. In this phase, the small filler particles can act as spacers, increasing the free volume and the gap between the polymer chains, thereby facilitating chain movement and reducing viscosity. However, as the concentration of the additive increases beyond a specific threshold, this effect is overcome. The saturation of the interpolymeric space and the physical obstruction caused by the large volume of particles decreases the overall mobility of the polymer chains, leading to a significant increase in viscosity and a consequent reduction in the MFR.

In contrast to reports, this study found no measurable differences in MFR of HDPE and PP composites with increasing additions of SP or BS. The absence of significant changes suggests that, at the concentrations analyzed, these residues are well dispersed within the polymer matrices without altering chain mobility or imposing major processing constraints. This stability in MFR is particularly advantageous for packaging applications, where consistent rheological behavior is essential for processes such as extrusion and molding. These findings emphasize the potential of SP and BS as sustainable reinforcements that do not negatively affect processability, even at higher loadings.

3.1.4 *Air permeability test*

In the air permeability test, firstly, the reference standard was validated by the equipment (green signal), obtaining a value corresponding to the standard of 406 L/m^2·s. The virgin HDPE presented an average air permeability of 25.60 ± 9.21 L/m^2·s and the virgin PP of 1.04 ± 0.88 L/m^2·s, being the only ones to obtain positive validation (green signal) by the equipment. The samples incorporating SP and BS (5, 10, 20 and 30%) showed even lower values, in many cases without any measurable flux (0 L/m^2·s), all of which obtained red signal, thus the values obtained cannot be accepted as they are considered null. These results indicate that the addition of SP to HDPE and PP formulations decreased air permeability, giving the formulations a nearly complete airflow barrier. However, the standard used specifies the method for measuring air permeability but does not define acceptance limits. Nevertheless, based on current technical classifications, values below 10 L/m^2·s are often considered characteristic of air-impermeable materials. Therefore, the results obtained indicate that formulations incorporating endogenous resources may be suitable for applications where a drastic reduction in permeability is required, such as technical barriers, packaging, or insulation. Some authors also report on the positive effect of mineral fillers on air permeability. Pannirselvam et al.[25] reported a 40% reduction in oxygen permeability upon the incorporation of 4% v. of organoclay into polyethylene. Also, Avella et al.[26] suggested that the calcium carbonate nanoparticles drastically reduced the permeability of oxygen and carbon dioxide for PP nanocomposites.

This result is highly promising for the packaging industry, as it enables the incorporation of residues, supporting a circular economy, while also enhancing a critical property as air permeability.

3.1.5 *Water vapor transmission rate*

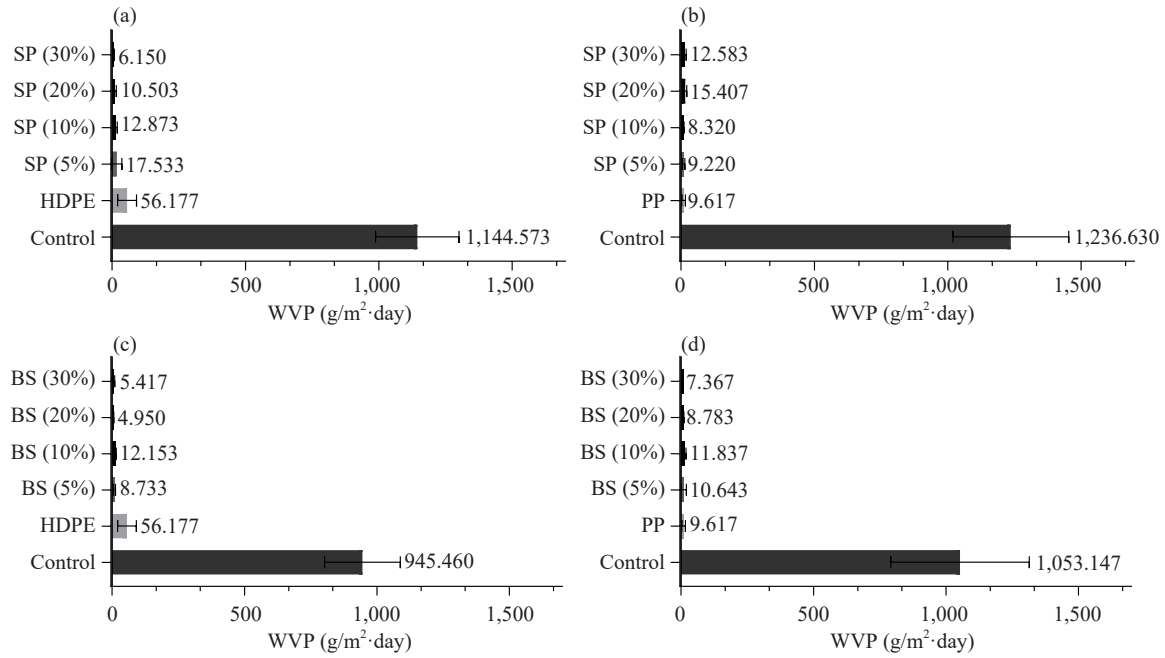

Figure 8. Water vapor permeability (g/m^2·day) for different formulations of PP and HDPE with and without reinforcement in 5, 10, 20 and 30% (w/w) of a) HDPE with Slate Powder(SP); b) PP with SP; c) HDPE with Bivalve Shells (BS) and d) PP with BS. Values are the mean ± SD (n = 3). Statistical analysis was performed between reinforced samples and polymers using ordinary one-way ANOVA Šídák's multiple comparisons test

The Water Vapor Permeability (WVP) test allows us to evaluate the performance of the different materials tested regarding their effectiveness as moisture barriers, with a view to their application in packaging. Figure 8 shows the water vapor permeability values ($g/m^2 \cdot day$) for the different formulations obtained in this work. The formulations are compared with their respective unreinforced polymers and with a high-permeability control fabric, used as a reference.

Statistical analysis shows no significant differences between reinforced HDPE and PP and virgin polymers. Although some discussion is possible to do considering the small values obtained for WVP. For HDPE, incorporation of SP progressively reduced the medium value of WVP from 56.17 $g/m^2 \cdot day$ for virgin HDPE to 17.53, 12.87, 10.50, and 6.15 $g/m^2 \cdot day$ at 5, 10, 20, and 30% SP, respectively (Figure 8a). This demonstrates the barrier effect of SP, which increases the tortuosity of water vapor diffusion paths. Similarly, BS reduced HDPE WVP from 56.17 $g/m^2 \cdot day$ to 8.73, 12.15, 4.95, and 5.41 $g/m^2 \cdot day$ at 5, 10, 20, and 30% BS, confirming its efficiency as a reinforcing agent with comparable or slightly superior barrier properties to SP (Figure 8c).

For PP, the effect is less pronounced. SP reduced WVP slightly up to 10% (9.22 and 8.32 $g/m^2 \cdot day$ for 5 and 10% SP) but increased at 20% (15.41 $g/m^2 \cdot day$) compared to virgin PP (9.62 $g/m^2 \cdot day$) (Figure 8b). BS showed modest reductions ranging from 10.64 to 7.37 $g/m^2 \cdot day$ for 5-30% addition (Figure 8d). Although the effect in PP is smaller than in HDPE, all formulations remained much less permeable than the reference fabric (1,236.63 $g/m^2 \cdot day$), demonstrating that even small amounts of mineral fillers contribute to the barrier effect.

Lightbody et al.[27] referenced, in a patent, that calcium carbonate, particularly in its nano form, has been demonstrated to significantly lower water vapor transmission rates in HDPE films, making them suitable for packaging applications that require moisture control. According to Zhang et al.,[28] introducing inorganic fillers or fibers into HDPE can improve the barrier properties against water vapor by creating a more complex channel for vapor to cross.

The addition of SP and BS improved the water vapor barrier performance of HDPE and PP composites. In HDPE, WVP decreased progressively with increasing filler content, with BS achieving slightly superior results compared to SP, confirming their effectiveness as reinforcing agents. In PP, the effect was more moderate. SP reduced permeability at low concentrations but increased it at higher loadings, while BS provided consistent improvements across all concentrations. Importantly, all filled formulations, for both polymers, exhibited WVP values below the reference fabric, demonstrating that even small amounts of these mineral fillers can significantly enhance barrier properties and support their potential use in sustainable packaging applications.

Overall, both SP and BS effectively reduce water vapor permeability in the two polymers. Their incorporation enhances the possibility of packaging application performance while supporting sustainability, as they are derived from recycled waste and renewable polymers.

3.1.6 *UV-radiation permeability test*

To evaluate the permeability of the different formulations to UV-radiation, transmittance (%) was measured in the 280-400 nm range (Figure 9).

Figure 9 shows that the permeability to UV radiation decreased as the amount of SP or BS increases, resulting in lower transmittance (%) across the entire measured wavelength range. HDPE formulations exhibited lower transmittance than PP, with maximum values of transmittance at 30% for HDPE and 65% for PP.

In HDPE formulations (Figures 9a and 9c), SP reinforcement appears to be more efficient than BS reinforcement in terms of UV permeability, since transmittance drops close to 0% at just 5% of SP while the same result with BS is only achieved at 30%. A similar behavior is observed for PP (Figures 9b and 9d), with 5% of SP reducing transmittance to nearly 0%, whereas BS required 30% to achieve the same outcome. In summary, SP was highly efficient in blocking UV radiation even at low concentrations, while BS achieved a similar performance but only at higher loadings (30%).

The reduction in UV transmittance observed with the incorporation of SP and BS aligns with previous reports. He et al.[29] incorporated nine types of natural minerals into polypropylene films and demonstrated that even at 2% loading, the additives significantly improved UV protection. Also, Dulíková et al.[30] investigated the shielding effect of nano-$CaCO_3$ in polypropylene fibers and showed that its incorporation, depending on content and processing, reduced UV transmission.

The outstanding performance of SP at low additions underscores its potential as a cost-effective and environmentally friendly reinforcement for packaging applications. Achieving complete UV blocking at such low concentrations not only enhances material functionality but also maintains processability and mechanical balance.

These findings show a significant development in the production of polymer composites with functional and protective properties.

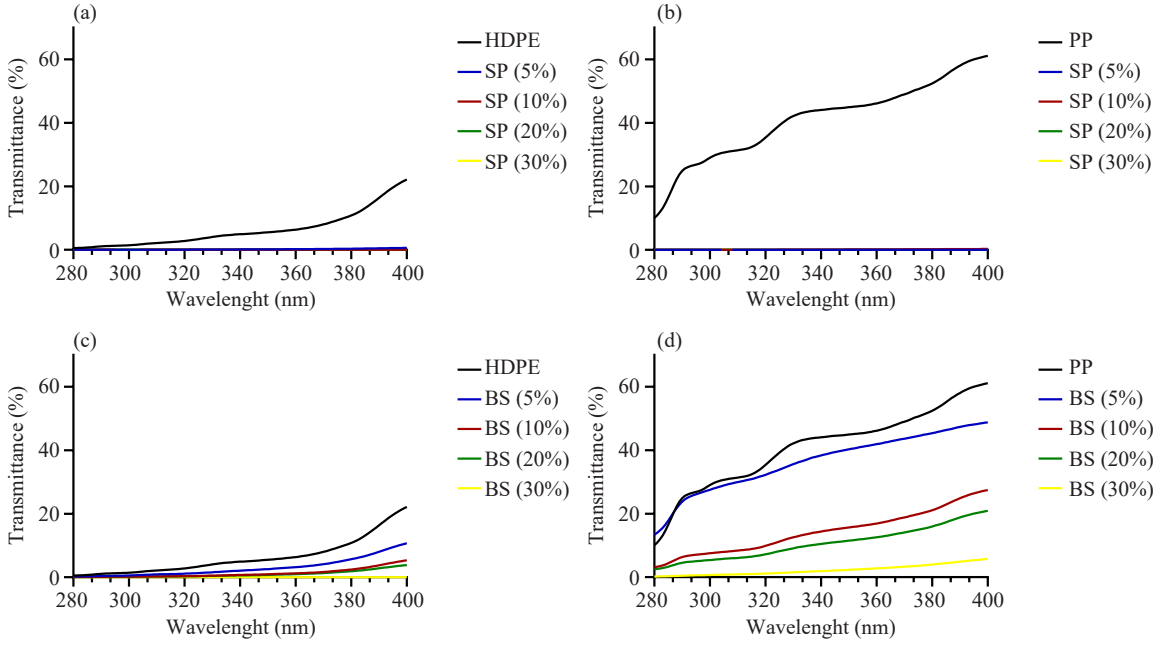

Figure 9. Transmittance (%) for different formulations of PP and HDPE with and without reinforcement in 5, 10, 20 and 30% (w/w) of Slate Powder (SP) and Bivalve Shells (BS) from 280 nm to 400 nm. a) HDPE with SP; b) PP with SP; c) HDPE with BS and d) PP with BS

3.2 *SEM analysis*

To better understand the mechanical and barrier behavior observed in the composites, SEM was performed on selected fractured samples (Figure 10). The analyzed formulations were intentionally chosen to represent the virgin polymers (HDPE and PP) and composites with filler contents that showed the most representative trends in the mechanical and permeability results. Intermediate and high filler loadings were selected, as these compositions exhibited significant differences in stiffness, permeability reduction, and UV shielding performance. SEM analysis of the fracture zones provides insight into filler dispersion, matrix-filler interfacial adhesion, and fracture mechanisms, which are key factors governing the balance between mechanical integrity, processability, and barrier efficiency in polyolefin-based composites reinforced with mineral residues.

Figure 10 provides important microstructural evidence that supports and explains the mechanical and barrier results previously discussed. The fracture surface of neat HDPE (Figure 10a) exhibits a relatively homogeneous and ductile morphology, characterized by rough surfaces and plastic deformation features, typical of polyolefins with good toughness. After incorporation of 20% SP (Figure 10b), the fracture surface becomes slightly more irregular, with well-dispersed mineral particles embedded in the matrix and no evident large voids or particle pull-out. This good dispersion and interfacial adhesion help explain why the addition of slate did not significantly alter the mechanical properties or melt flow behavior, while still promoting a strong barrier effect by increasing diffusion tortuosity.

In contrast, HDPE with 30% of Bivalve Shells (BS) (Figure 10c) shows more pronounced rigid inclusions, consistent with the high $CaCO_3$ content in BS. The presence of angular particles and localized stress concentration zones explains the observed increase in stiffness (Young's modulus) and the enhanced barrier performance, but also suggests a more brittle fracture mechanism compared to neat HDPE and HDPE/SP. These morphological features are in line with the reduced permeability values and the stiffer mechanical response observed for BS-reinforced HDPE.

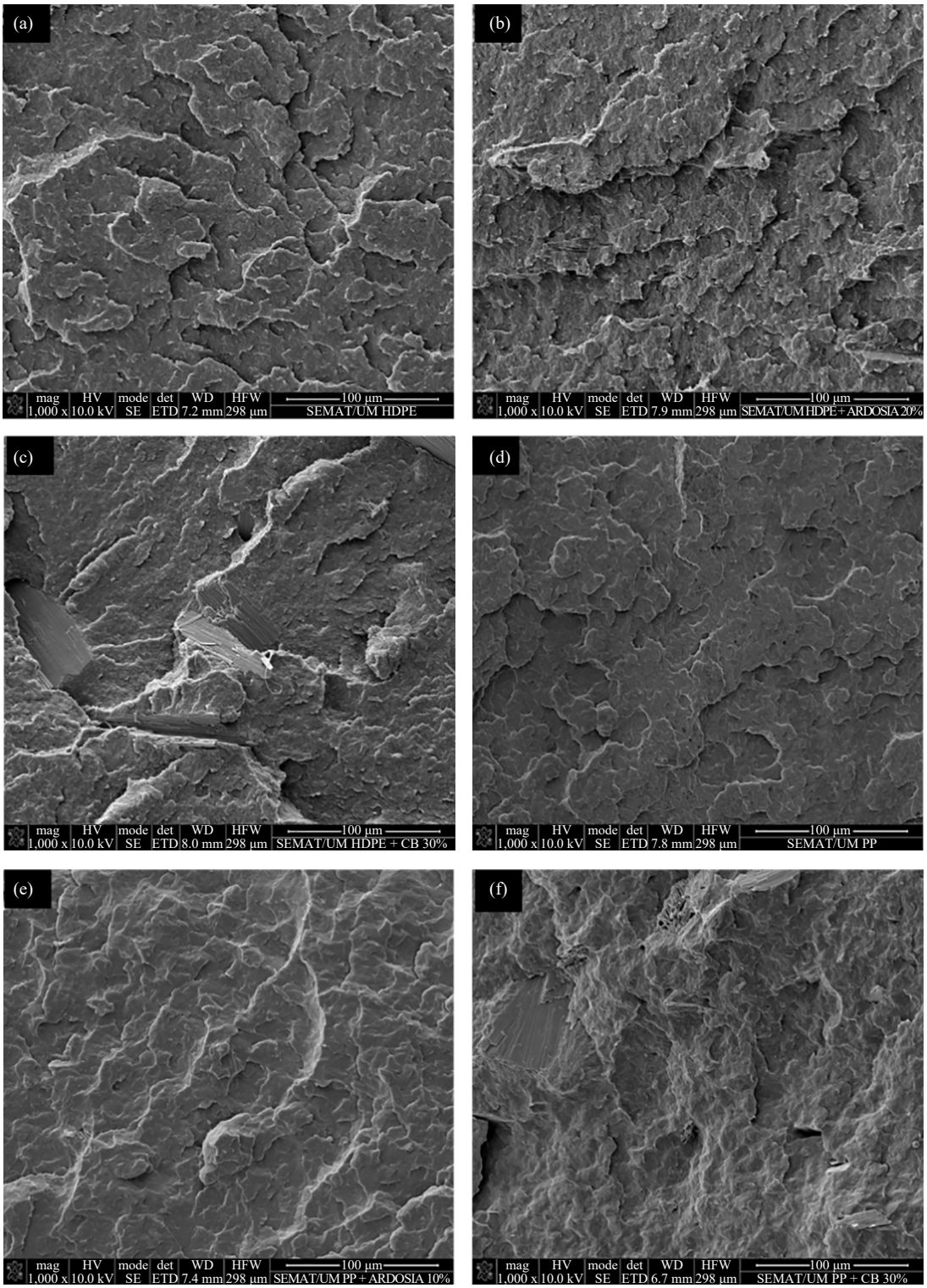

Figure 10. SEM micrographs of the samples fracture zone: a) HDPE; b) HDPE with 20% of Slate Powder (SP); c) HDPE with 30% of Bivalve Shells (BS); d) PP; e) PP with 10% of SP; and f) PP with 30% of BS

For PP, virgin PP (Figure 10d) displays a smoother fracture surface, indicative of lower ductility compared to HDPE. With the addition of 10% of SP (Figure 10e), the fracture morphology remains relatively uniform, and the filler appears well integrated into the polymer matrix. This observation correlates with the minor changes in mechanical

and barrier properties reported for PP/SP systems, confirming that slate does not strongly disrupt PP's structural integrity at low to moderate loadings. At higher BS content (30%, Figure 10f), the PP matrix shows a rougher and more heterogeneous fracture surface, with visible filler agglomerates and microvoids. These features may account for the modest and less consistent improvements in permeability and the limited mechanical reinforcement observed in PP compared to HDPE.

Overall, the SEM analysis confirms that the effectiveness of SP and BS as reinforcements is strongly dependent on polymer type and filler content. The good dispersion and interfacial compatibility observed particularly in HDPE-based composites explain the significant improvements in barrier performance without detrimental effects on processability. In PP systems, the more limited interaction between filler and matrix helps justify the less pronounced improvements. These microstructural observations reinforce the conclusion that recycled HDPE is especially well suited for valorization with SP and BS residues, enabling enhanced performance while maintaining mechanical integrity and sustainability.

3.3 *FTIR analysis*

FTIR was conducted to evaluate the chemical structure of HDPE and PP composites and to investigate potential interactions between the polymer matrices and the mineral fillers (Figure 11). In accordance with SEM analysis, the selected samples correspond to the formulations that exhibited the most representative mechanical and barrier behaviors. FTIR provides insight into whether the improvements in barrier properties, UV shielding, and mechanical performance are associated with chemical interactions or are primarily driven by the physical presence and dispersion of the fillers. By comparing the spectra of virgin polymers, fillers, and their composites, it is possible to assess the preservation of the polymer backbone, identify characteristic mineral vibrations, and correlate the chemical and structural information with the morphological observations obtained from SEM and the functional results for permeability, stiffness, and processability.

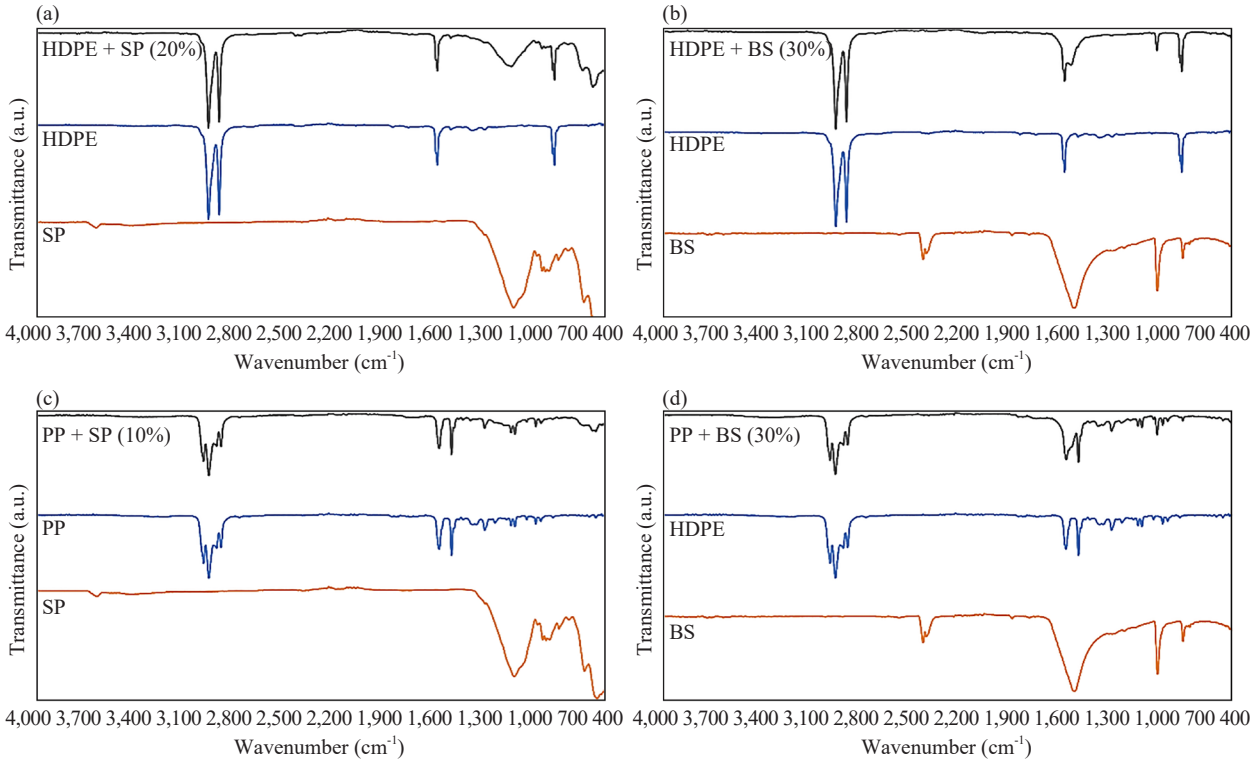

Figure 11. FTIR spectra of the different formulations compared with the respective virgin polymer and filler

The FTIR spectra presented in Figure 11 provide complementary chemical information that supports the mechanical, barrier, and morphological results. The spectra of virgin HDPE and PP display the characteristic polyolefin bands, including C-H stretching vibrations at approximately 2,915 and 2,848 cm^{-1}, bending modes near 1,470-1,460 cm^{-1}, and rocking vibrations around 720-730 cm^{-1}, which remain clearly identifiable in all composites. This confirms that the polymer backbone is preserved after the incorporation of SP and BS, in agreement with the unchanged melt flow rate and mechanical integrity observed.

For the composites containing SP, additional absorption features appear below 1,200 cm^{-1}, attributable to Si-O-Si and Al-O vibrations of the silicate-rich filler. The presence of these peaks, without significant shifts in the polymer characteristic bands, indicates that SP interacts with the polymer predominantly through physical interactions at the interface rather than chemical bonding. This observation, together with the SEM evidence of uniform filler dispersion, supports that interfacial adhesion is sufficient to transfer stress and increase tortuosity for barrier improvement and UV shielding, while preserving mechanical integrity.

Similarly, BS-reinforced composites show characteristic carbonate bands near 1,400-1,450 cm^{-1} and 870 cm^{-1}, confirming the presence of $CaCO_3$. Again, the absence of new chemical bands or shifts in polymer peaks indicates that BS acts as an inert filler, yet its presence at the interface contributes to increased stiffness and improved barrier properties by physically constraining polymer chain mobility.

Overall, the FTIR analysis, when interpreted alongside SEM observations, confirms that the enhancements in mechanical stiffness, water vapor and air permeability, and UV shielding are driven by the physical presence, dispersion, and interfacial interactions of the mineral fillers, rather than chemical modification of the polymer. This provides a mechanistic basis for the observed composition-structure-performance relationships and reinforces the suitability of SP and BS residues as sustainable reinforcements for recycled HDPE and renewable PP.

3.4 *Proof of concept*

This section focusses on evaluating the feasibility of producing bottles using HDPE and PP formulations reinforced with SP and BS (Figure 12). Preliminary experiments were performed to assess structural integrity, processability, and surface characteristics of the reinforced polymers. The findings provide insight into the potential of these sustainable formulations for extrusion-blow molding applications, while highlighting trends in material performance and surface properties.

Figure 12. Demonstration of the feasibility of the application proposed

Figure 12 shows representative bottles produced from the reinforced HDPE and PP formulations. The image clearly demonstrates that the formulations can be successfully processed via blow-extrusion, resulting in bottles with consistent shape and structural integrity. Despite the addition of SP and BS fillers, no major defects, warping, or surface irregularities were observed, indicating that the reinforcements are compatible with the manufacturing process. These

observations provide clear proof of concept, confirming that the developed formulations are suitable for producing functional bottles and supporting further investigations into their physical and surface properties.

4. Conclusions

This study demonstrated that Slate Powder (SP) and Bivalve Shells (BS) effectively reinforce recycled HDPE and renewable PP, enhancing barrier, UV-shielding, and mechanical properties in a sustainable way. Water vapor permeability in HDPE decreased from 56.17 to 6.15 g/m^2·day (30% SP) and 4.95 g/m^2·day (20% BS), while air permeability and UV transmittance were also significantly reduced, with near-complete UV blocking at 5% SP and 30% BS. Mechanically, BS increased Young's modulus, whereas SP preserved flexibility and processability. SEM and FTIR analyses confirmed good filler dispersion and the integrity of the polymer matrix, indicating that improvements arise from physical reinforcement. The most promising formulations, HDPE + SP (20%), HDPE + BS (30%), PP + SP (10%), and PP + BS (30%), are suitable for blow extrusion-based packaging. Although, future studies will examine the fabricating of the bottles and assess their potential for reuse and long-term durability.

Overall, these results highlight the potential of industrial and biological mineral residues to valorize recycled and renewable polymers, producing high-performance composites that support circular economy strategies.

Funding

This research was funded by the Portugal 2030 Program, under the project EcoNanoPackaging (No. 14449), represented by the code CENTRO2030.

Conflicts of interest

The authors declare no competing financial interest.

References

[1] Wang, L.; Elahi, E.; Zhou, Y.; Wang, L.; Zhang, S. A review of packaging materials' consumption regulation and pollution control. *Sustainability* **2022,** *14*(23), 15866.

[2] Hussain, M. A.; Mishra, S.; Agrawal, Y.; Rathore, D.; Chokshi, N. P. A comparative review of biodegradable and conventional plastic packaging. *Interactions* **2024,** *245*(1), 1-26.

[3] Segura-Méndez, K. L.; Puente-Córdova, J. G.; Rentería-Baltiérrez, F. Y.; Luna-Martínez, J. F.; Mohamed-Noriega, N. Modeling of stress relaxation behavior in HDPE and PP using fractional derivatives. *Polymers* **2025,** *17*(4), 453.

[4] Hendrawati; Liandi, A. R.; Solehah, M.; Setyono, M. H.; Aziz, I.; Siregar, Y. D. I. Pyrolysis of PP and HDPE from plastic packaging waste into liquid hydrocarbons using natural zeolite lampung as a catalyst. *Case Stud. Chem. Environ. Eng.* **2023,** *7*, 100290.

[5] Samuel, H. S.; Ekpan, F.-D. M.; Ori, M. O. Biodegradable, recyclable, and renewable polymers as alternatives to traditional petroleum-based plastics. *Asian J. Environ. Res.* **2024,** *1*(3), 152-165.

[6] Taurino, R.; Bondioli, F.; Messori, M. Use of different kinds of waste in the construction of new polymer composites: Review. *Mater. Today Sustain.* **2023,** *21*, 100298.

[7] Tong, J.; Yu, S.; Yao, Z.; Jiang, J.; Lu, H.; Zhou, Y. G.; Yang, H.; Wen, Z. Preparing polyethylene composites using nonmetallic fractions derived from waste printed circuit boards and shellfish waste: Toward synergistic waste utilization and circular economy. *Circ. Econ.* **2024,** *3*(1), 100073.

[8] Frías, M.; Vigil de la Villa, R.; García, R.; de Soto, I.; Medina, C.; Sánchez de Rojas, M. I. Scientific and technical aspects of blended cement matrices containing activated slate wastes. *Cem. Concr. Compos.* **2014,** *48*, 19-25.

[9] Giordano, L.; Ferraro, L.; Caroppo, C.; Rubino, F.; Buonocunto, F. P.; Maddalena, P. A method for bivalve shells characterization by FT-IR photoacoustic spectroscopy as a tool for environmental studies. *MethodsX* **2022,** *9*,

101672.
[10] Yoon, G. L.; Kim, B. T.; Kim, B. O.; Han, S. H. Chemical-mechanical characteristics of crushed oyster-shell. *Waste Manage.* **2003,** *23*(9), 825-834.
[11] Silva, D.; Debacher, N. A.; De Castilhos, A. B.; Rohers, F. Caracterização físico-química e microestrutural de conchas de moluscos bivalves provenientes de cultivos da região litorânea da Ilha de Santa Catarina [Physicochemical and microstructural characterization of bivalve mollusk shells from aquaculture in the coastal region of Santa Catarina Island]. *Quim. Nova* **2010,** *33*(5), 1053-1058.
[12] International Organization for Standardization. *ISO 527-2:2012: Plastics—Determination of Tensile Properties—Part 2: Test Conditions for Moulding and Extrusion Plastics*; ISO: Geneva, 2012.
[13] International Organization for Standardization. *ISO 178:2019: Plastics—Determination of Flexural Properties*; ISO: Geneva, 2019.
[14] International Organization for Standardization. *ISO 1133-1:2022: Plastics—Determination of the Melt Mass-Flow Rate(MFR) and Melt Volume-Flow Rate(MVR) of Thermoplastics—Part 1: Standard Method*; ISO: Geneva, 2022.
[15] Pais, V.; Silva, P.; Bessa, J.; Dias, H.; Duarte, M. H.; Cunha, F.; Fangueiro, R. Low-velocity impact response of auxetic seamless knits combined with non-Newtonian fluids. *Polymers* **2022,** *14*(10), 2065.
[16] ASTM International. *ASTM E96/E96M-14: Standard Test Methods for Water Vapor Transmission of Materials*; ASTM International: West Conshohocken, PA, 2014.
[17] ASTM International. *ASTM E903-20: Standard Test Method for Solar Absorptance, Reflectance, and Transmittance of Materials Using Integrating Spheres*; ASTM International: West Conshohocken, PA, 2020.
[18] Carbonell-Verdú, A.; García-García, D.; Jordá, A.; Samper, M. D.; Balart, R. Development of slate fiber reinforced high density polyethylene composites for injection molding. *Compos. Part B Eng.* **2015,** *69*, 460-466.
[19] Webb, C.; Qi, K.; Anguilano, L.; Schmidt Rivera, X. Mechanical and environmental evaluation of ground calcium carbonate($CaCO_3$) filled polypropylene composites as a sustainable alternative to virgin polypropylene. *Results Mater.* **2024,** *22*, 100562.
[20] Lapčík, L.; Maňas, D.; Vašina, M.; Lapčíková, B.; Řezníček, M.; Zádrapa, P. High density poly(ethylene)/$CaCO_3$ hollow spheres composites for technical applications. *Compos. Part B Eng.* **2017,** *113*, 218-224.
[21] Tirlangi, S.; Jinnah Sheik Mohamed, M.; Karthik, K.; MohanDas Gandhi, A. G.; Thiruselvam, K.; Rajesh Kumar, E. Influence on the mechanical properties of virgin recycled polypropylene composites with different types of reinforcing loads. *Mater. Today Proc.* **2023**. https://doi.org/10.1016/j.matpr.2023.07.235 (accessed Jan 20, 2026).
[22] Peng, Y.; Musah, M.; Via, B.; Wang, X. Calcium carbonate particles filled homopolymer polypropylene at different loading levels: Mechanical properties characterization and materials failure analysis. *J. Compos. Sci.* **2021,** *5*(11), 302.
[23] Liang, J. Z.; Zhu, Z. H. Research into melt flow properties of polypropylene/diatomite composites. *J. Reinf. Plast. Compos.* **2010,** *29*(10), 1580-1589.
[24] Benz, J.; Bonten, C. R. Rigid amorphous fraction caused by particle-polymer interaction in highly filled plastics. *AIP Conf. Proc.* **2020,** *2289*(1), 020012.
[25] Pannirselvam, M.; Genovese, A.; Jollands, M. C.; Bhattacharya, S. N.; Shanks, R. A. Oxygen barrier property of polypropylene-polyether treated clay nanocomposite. *Express Polym. Lett.* **2008,** *2*(6), 429-439.
[26] Avella, M.; Cosco, S.; Di Lorenzo, M. L.; Di Pace, E.; Errico, M. E.; Gentile, G. iPP-based nanocomposites filled with calcium carbonate nanoparticles: Structure/properties relationships. *Macromol. Symp.* **2006,** *234*(1), 156-162.
[27] Lightbody, O. C.; Chisholm, P. S.; Aubee, N. D. J.; Tikuisis, T. Improved Barrier Properties of HDPE Film. CA Patent 2759953 A1, Nov 28, 2011.
[28] Zhang, D.; Guo, M.; Pan, G.; Miao, Z.; Liu, Y. Methods of improving barrier properties of HDPE. *China Synth. Resin Plast.* **2011,** *28*(5), 68-72.
[29] He, P.; Low, R. J. Y.; Burns, S. F.; Lipik, V.; Tok, A. I. Y. Enhanced far infrared emissivity, UV protection and near-infrared shielding of polypropylene composites via incorporation of natural mineral for functional fabric development. *Sci. Rep.* **2023,** *13*(1), 1-12.
[30] Dulíková, M.; Strecká, Z.; Ujhelyiová, A.; Legéň, J.; Bugaj, P. Shielding effect of nanoadditives against UV radiation in polypropylene fibres. *Fibres Text. East. Eur.* **2010,** *18*(5), 82.